ARTICLE OPEN

Check for updates

Actinides and fission products in reactor graphite after loss-of-flow accident

Alexander O. Pavlyuk[1], Sergei G. Kotlyarevskii[1], Roman I. Kan[1], Anna G. Volkova[2], Vasiliy O. Yapaskurt[3], Elena V. Zakharova[2] and Andrei A. Shiryaev[2]✉

Samples of irradiated graphite from a uranium-graphite reactor contaminated with fuel debris from loss-of-flow accidents, are investigated. Peculiarities of spatial distribution, speciation, and kinetics of leaching by aqueous solution of actinides and fission products are studied at scales from the whole reactor stack down to sub-mm graphite fragments. The main fraction of fuel debris is associated with aluminosilicate-based phases decorating cracks and other defects of damaged graphite details. Elemental composition of actinides and fission products depends on both irradiation and leaching conditions. Significant differences are observed between leach kinetics of various radionuclides; integral leached fraction varies between ~5% for ^{244}Cm to ~90% for ^{134,137}Cs. For some radionuclides sudden massive release due to uneven dissolution of the carrier phases is observed. Disposal of irradiated graphite with significant fraction of fuel debris requires dedicated treatment aimed either at decontamination or at conversion of the radionuclides to insoluble well-fixed form.

npj Materials Degradation (2022)6:23 ; https://doi.org/10.1038/s41529-022-00235-3

INTRODUCTION

Graphite-moderated reactors constitute a significant share of operational and stopped nuclear reactors. Decommissioning of these reactors requires detailed understanding of distribution and speciation of radionuclides present in irradiated graphite (i-graphite). Considerable amount of studies address behavior of ^{14}C and ^{36}Cl in i-graphite, i.e., radionuclides produced by activation of carbon, nitrogen, and lattice impurities[1–7]. However, during various accidents reactor graphite may also be contaminated by fuel debris comprising actinides and fission products (FP). They enter the stack during eventual local contacts between the graphite blocks and fuel and are subsequently dispersed and spread in the core by coolant flow. Following cooling period of 5–10 years after the reactor shutdown, radioactivity of the contaminated graphite is primarily determined by FP (^{137}Cs, ^{90}Sr, ^{152,154,155}Eu) and actinides (isotopes of U, Np, Pu, Am, and Cm) produced from the fuel debris[7–10]. At present, the largest amount of fuel debris in a single graphite clad—up to 15 tonnes – is located in the Windscale Pile No. 1 (UK) damaged by fire in 1957[11]. Although relative volume of graphite contaminated by fuel debris is not very important (in Russia it is estimated as ~3000 tonnes or ~5% of the total amount[8–10,12]), its high radioactivity complicates handling and requires development of novel approaches for handling and disposal[13].

In most reactors, loss-of-coolant accidents (LOCA) are the main source of fuel debris in the i-graphite. Clogging of a channel or appearance of leaks may drastically decrease the efficiency of the heat removal from fuel due to partial or complete loss of the coolant flow. In normal operation, the temperature of graphite is ~600–650 °C (case of RBMK-type reactor), but in the LOCA events it may locally raise to ~1000 °C. In case of metallic fuel such temperatures may induce melting and chemical interaction with the cladding and technological channels. Resulting corium is heated up to ~1500–1800 °C[14]. Since the gas mixture (usually N_2 or He–N_2) surrounding the graphite clad is only slightly overpressurized, the fuel debris from damaged rods may contact the graphite stacks. If the accident occurs when a reactor operates at full power, interaction of the coolant (such as superheated water) with graphite blocks and molten corium leads to steam formation and dispersal of fuel fragments, corium and by-products of their interaction in the stack. Accidents at RBMK reactors at Leningrad NPP in 1975 and at 3rd block of Chernobyl NPP in 1982 exemplify such events[15].

In most cases, the fuel fragments will be deposited in the vicinity of the accident spot due to flow stagnation and formation of extensive open porosity and caverns in graphite by steam oxidation. In course of post-accident maintenance, the main fraction of fuel debris localized in the damaged technological channel is removed using mechanical tools, purging with pressurized gases and liquids, etc. However, complete cleaning is impossible without full dismantling of the graphite stack. The residues are further irradiated during subsequent operation of the reactor and, in addition, participate in thermochemical processes including interaction with the coolant and decontamination agents. Subsequently, a very complex pattern of distribution and speciation of radionuclides and stable isotopes, partly influenced by volatility of radionuclides and their solubility in the coolant, is formed in the graphite stack. Although this information is required for dismantling of the reactors and eventual decontamination of the graphite, at present little is known about state of nuclear fuel debris in damaged graphite.

In this work, we present results of comprehensive investigation of graphite extracted from a closed graphite-moderated reactor. Using complementary approaches accessing widely different scales—from the whole graphite stack down to sub-mm chips—we analyze spatial distribution and speciation of radionuclides and selected stable isotopes. Leaching behavior of relevant radionuclides in model ground water of proposed underground

[1]Pilot and Demonstration Center for Decommissioning of Uranium-Graphite Nuclear Reactors, Autodoroga 13, Bld. 179A, Seversk, Tomsk oblast 636000, Russia. [2]Frumkin Institute of Physical Chemistry and Electrochemistry, Russian Academy of Sciences, Leninsky pr., 31 korp. 4, Moscow 119071, Russia. [3]Department of Geology, Lomonosov Moscow State University, Moscow 119991, Russia. ✉email: shiryaev@phyche.ac.ru

repository was studied. Main phases comprising actinides and FP derived from fuel debris are identified. Unless explicitly indicated, in this paper under term radionuclides only FP and actinides are considered.

RESULTS

Distribution of radionuclides in reactor stack

The graphite-moderated reactor studied in this work operated with unenriched metallic uranium fuel in Al-alloys cladding. In early period of the reactor operation, a loss-of-flow (LOF) accident took place. Due to perforation of a cladding, fuel and clad corrosion products accumulated in the fuel rod and caused its expansion. Resulting blockage of the coolant flow led to overheating and melting of fuel, cladding and walls of the technological channel, allowing contact of the corium with the graphite blocks and contamination of the stack with fuel debris.

Distribution of "hot" spots in the entire graphite stack was studied using neutron and, subsequently γ-scanning to determine exact locations of fuel debris agglomerates (Fig. 1). Figure 1a shows distribution of radionuclides in the graphite stack as obtained by neutron scanning. "Hot" spots and related haloes are clearly observed. In most damaged channels distribution of radionuclides is markedly heterogeneous both in vertical direction (along the channel) and in the graphite block cross-section, typical γ-profile is shown in Fig. 1b. Activity maxima correspond to joints between the graphite blocks (Fig. 1b, c). Such distribution shows that in most cases only the damaged channel is heavily contaminated and the post-accident cleaning allowed removal of major part of the damaged fuel with exception of debris, which penetrated into contacts between the graphite blocks, see below. A dedicated device (Fig. 1c) allowed selection of a point of interest using a videocamera (Fig. 1d) and sampling of the graphite (Fig. 1e).

Typical distribution of radionuclides across the individual graphite block situated at the accident spot is shown in Fig. 2 (see also ref. [5]); results for a block located approximately 1 m from this site are shown for comparison. On the scale of individual graphite details (blocks, rings, and sleeves) the highest content of radionuclides is observed on external and internal surfaces.

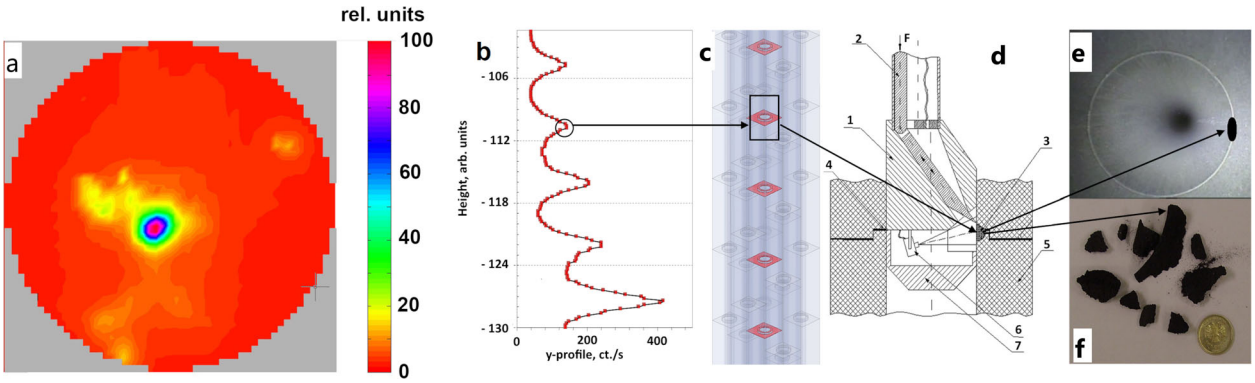

Fig. 1 Spatial distribution of "hot" spots due to fuel debris in the reactor pile and sampling device. A Neutron emission map in horizontal plane of the reactor stack, diameter of the stack is ~9 m. **B**, **C** Typical vertical γ-profile along technological channel, maxima of γ-activity correspond to joints between graphite blocks. **D** The sampling device: 1—body, 2—movable rod allowing chisel operations, 3—chisel contact with a contaminated area, 4—joint between graphite blocks, 5—graphite block, 6—videocamera, 7—sample collector. **E** Camera view of the channel walls with a joint between the graphite blocks. **F** Pieces of graphite extracted from the damaged channel (the coin diameter is 22 mm).

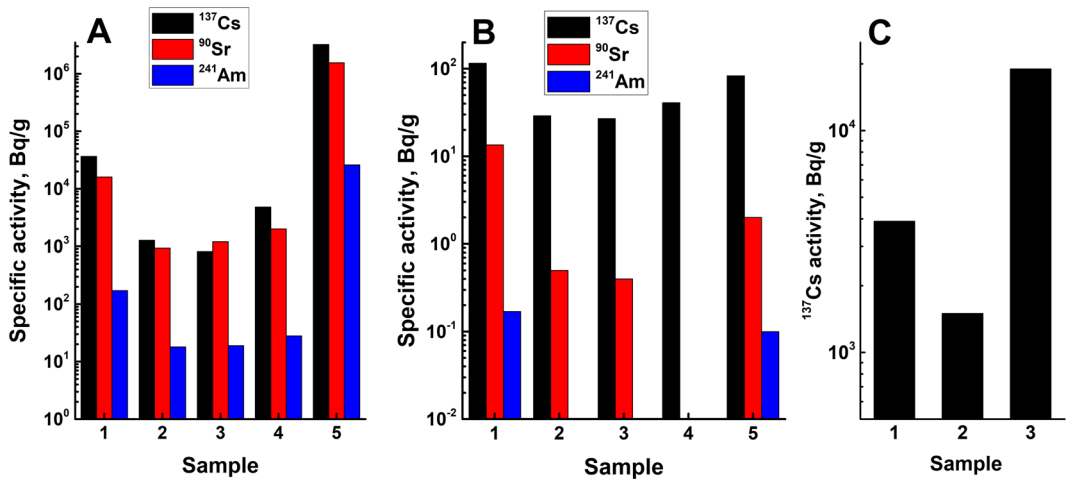

Fig. 2 Distribution of some fuel-related radionuclides in cross-section of the graphite block as studied after the reactor shutdown. A Graphite block directly affected by the LOF accident. B Block distant from the accident spot. **C** Graphite sleeve irradiated only in the three final years of the reactor operation, total sleeve thickness—20 mm. No actinides are detected in the sleeve. In **A**, **B**, point 1 is at the contact between the internal borehole in the graphite block and the sleeve, point 5—outer surface of the block. In **C**, point 1 is at the contact with technological channel, point 3—outer edge of the sleeve (contact with graphite block).

Penetration into the graphite bulk is possible for FPs, but is much less pronounced for actinides. It is important to note that the tube of a technological channel is not in direct contact with the central borehole of a graphite block; they are separated by graphite spacer rings and sleeves. During decontamination operations after the accidents and in course of regular maintenance works the borehole is cleaned both mechanically and chemically, thus explaining reduced contamination on its walls. However, external surfaces of the graphite blocks are not decontaminated during these operations due to their close contact with other blocks, thus explaining patterns shown in Fig. 2a. Similar distribution patterns (in particular, of ^{137}Cs) were reported for graphite of destroyed fourth Unit of Chernobyl NPP[16]. In the latter case, dispersal of radionuclides in volatile form played major role, but contribution of transport by the coolant during early stages of the accident is also not excluded.

For comparison, Fig. 2b shows typical distribution of radionuclides in a graphite block, which was located in a different part of the core and was not affected by the accidents. Marked differences in amount of radionuclides in comparison with the accidental block are immediately obvious, although absolute radioactivity values are not insignificant and vary considerably. One might suggest that activation and fission of trace uranium and other impurities inherited from graphite production and from the coolant (filtered river water) contribute to the inventory of radionuclides. However, concentration of uranium in virgin GR-220 does not exceed 6.5×10^{-6} mass%, consequently, amount of ^{241}Am accumulated during the reactor lifetime will be less than 0.6 Bq/g; similar values will be observed for FPs[9,17,18]. As shown below, mineral impurities present in river water influence behavior of radionuclides from the fuel debris by formation of host phases. However, these minerals themselves do not affect considerably the total radioactivity of i-graphite. The coolant contains traces of natural minerals, which were not filtered from the incoming water and some amount of corrosion products of the construction materials of the reactor itself. Activation of Fe-compounds produces ^{60}Co and impurities in Al-alloys give rise to ^{152,154,155}Eu. Almost certainly, activation of the corrosion products is much more important radiologically. Distribution of ^{60}Co in cross-section of graphite blocks and sleeves is similar to those shown in Fig. 2 (see also ref. [6]), i.e., the major fraction reside on external surfaces. However, the total inventory of the coolant-related radionuclides is rather minor and the major fraction of detected contamination of the i-graphite with actinides and FPs is due to dispersed fuel debris from the accident spot. This hypothesis is supported by analysis of FPs in a graphite sleeve, which was installed just ~1 m away from the accident spot, but 20 years after it has occurred. Despite long period of safe operation, notable ^{137}Cs activity is present in the sleeve (Fig. 2c).

The major fraction of fuel debris from the LOF accident is confined to the affected technological channel. However, analysis of the distribution of radionuclides suggests that non-negligible share is transported by fluids and/or steam and penetrates into contacts between the graphite blocks and also enters open porosity of the graphite itself. Nuclear graphite is characterized by interconnected open porosity accessible for fluids and gases[19], which only moderately changes with irradiation[20]. Diffusion of radionuclides in the graphite bulk is expected to be much less important. Presumably, radionuclides in the volume of graphite details will mostly concentrate on walls of the pores, cracks and other internal defects. Investigation of the sleeve (Fig. 2c) shows that even despite thorough cleaning, the spot contaminated in the accident may serve as a source of radionuclides for long periods of time. At the same time, absence of actinides in the sleeve implies that only relatively mobile Cs can be relocated on long timescales and form extensive haloes around the damaged cells.

Properties of damaged graphite

Two types of samples extracted from the reactor several years after its final shutdown were studied (Supplementary Fig. 1): an entire graphite sleeve (Supplementary Fig. 1a) and a fragment of a graphite block (Supplementary Fig. 1b). The sleeve was irradiated for ~3 years in the end of the reactor operations. It was positioned approx. 1 m away from the location of an accident, which has occurred more than 20 years earlier. Despite large time interval after the accident, it is contaminated by FPs; no actinides were detected. Spatial distribution of FPs is shown in Fig. 2. In addition, graphite fragments of a block directly affected by the LOF accident were extracted from a horizontal joint between two graphite blocks. The fragments are heavily contaminated by the fuel debris, which were irradiated for many years after the accident. This type of samples is characterized by poor mechanical properties.

The studied graphite stack is made from GR-220 variety, which is virtually identical to the GR-280 employed in RBMK[21]. Changes in mechanical and thermal properties of GR-220 during irradiation are summarized in Table 1. Structural peculiarities and porosity changes with irradiation are described in refs. [20,22], respectively. Broad range of the values shown in Table 1 for irradiated graphite is due to strong influence of temperature and neutron flux on thermomechanical properties and significant variations of both parameters across the core.

Raman spectra were collected from virgin graphite and from a specimen contaminated by fuel debris (Fig. 3). Irradiation and steam oxidation lead to marked increase of the I(D)/I(G) ratio and broadening of the G peak in the later sample, indicating higher concentration of point defects and decrease of sizes of graphitic crystallites. Appearance of large number of defects is consistent with decreased thermal conductivity. In Raman spectra of the damaged sample an A-band centered at ~1480 cm^{-1} typical for highly disordered carbon and tentatively ascribed to deformation bands in vicinity of point defects and/or heteroatoms[23] is observed, but its intensity varies markedly from point to point. Since nuclear graphite consists of two major carbonaceous components—filler and binder—considerable scatter of Raman spectra recorded in different spots is not uncommon[20,24]. However, in the case of the studied damaged samples local variations were fairly small. Although the statistics is limited, one might assume that steam oxidation preferentially removed the

Table 1. Selected properties of GR-220 graphite.

Property	Virgin GR-220[a]	Irradiated	Irradiated and steam-oxidized in damaged channels[b]
Density, g/cm^3	1.65–1.7	1.6–1.7	1.2–1.4
Tensile strength, σ, MPa	$34_{\parallel}/33_{\perp}$	33–60	10–15
Thermal conductivity, λ, W/m·K	$103_{\parallel}/89_{\perp}$	15–25	8–10

[a]For the virgin graphite properties are given for directions parallel and perpendicular to the block axis.
[b]The lowest measured values for fragments preserving integrity; in many cases mechanical destruction of graphite into fine pieces is observed.
All measurements performed at 20 °C.

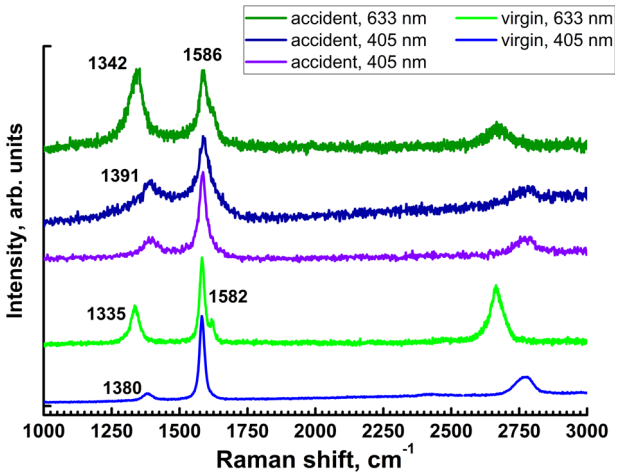

Fig. 3 Raman spectra of virgin GR-220 graphite and of the samples from fuel-contaminated volume. Spectra were recorded using 405 and 633 nm lasers; positions of D and G peaks is indicated. Spectra are displaced vertically for clarity.

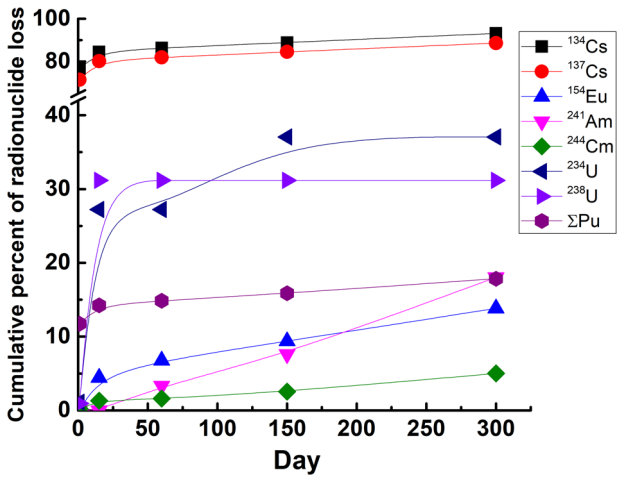

Fig. 4 Dynamics of leaching of fuel-related radionuclides. The sample of a block graphite was an irregular lump with mass 15.5 mg. The lines are drawn to guide an eye.

binder, generally characterized by poorer crystalline structure, which lead to reduced variability of the Raman spectra. Etching of the binder explains decrease of strength and mechanical disintegration of graphite blocks.

Distribution of radionuclides in graphite blocks and leaching

Investigation of radionuclides distribution in the graphite batches (see Supplementary Methods for methodology) shows that in the sleeve graphite ^{137}Cs from fuel debris is primarily present as a contamination on various surfaces (pores, faces of graphitic crystallites, etc.). In the mixed sample from both sleeves and blocks, "hot" particles, i.e., fuel debris, are present. Partial leaching of the fuel debris has obviously occurred during the accident progression when the radioactive halo around the damaged cell was formed. However, duration of these events was rather short (at most several hours), since the coolant leaks or clogging initiated prompt shutdown with subsequent drying of the stack. In normal operation, graphite is in nitrogen gas atmosphere. In the present work, leaching was investigated for samples extracted from a closed reactor several years after the shutdown and thus reflect processes occurring with "equilibrium" phases, i.e., formed in course of long-term irradiation at various temperatures and transient leaching.

Leaching behavior of selected radionuclides from the block graphite is presented in Fig. 4. The total leached fraction varies markedly between the radionuclides: from ~5% for ^{244}Cm to ~90% for ^{134,137}Cs. We note that fractions of the leached fuel-related isotopes are much larger in comparison with principal activation products ^{14}C and ^{36}Cl; for the later radionuclides <0.01% and <3%, respectively, were lost in 300 days-long experiment[25]. For most isotopes the largest losses are observed in the initial 15 days of the experiment, implying that these nuclides were present in soluble form or were adsorbed on easily soluble phases. In contrast, Np and Am isotopes were not detected in the first days of the leaching experiment suggesting that carrier phases were either inaccessible or are only weakly soluble. The leaching kinetics of different isotopes of elements such as Cs, Pu, and U are identical with measurement uncertainty.

At present permissible rates of radionuclide leaching from i-graphite are not yet described in Russian legislation. Intrinsic porosity of graphite complicates direct comparison of leach rates for i-graphite with monolithic waste forms[20,25]. It is important to emphasize that in the present work we report cumulative fraction of radionuclides, which can be leached from the graphite contaminated by fuel debris and not the leach rates. According to Russian regulation, i-graphite contaminated with fuel debris is grouped according to total content of long-living radionuclides (actinides and FPs) and materials with actinide content similar to that observed in the studied samples should be isolated in deep geological repository.

Fuel debris and related particles

Investigation of phase composition of fuel debris and related particles dispersed in graphite is important both from fundamental and decontamination/decommissioning points of view. Despite rather high radioactivity of block graphite samples, search for the debris particles proved to be difficult. At first, an attempt to locate them using digital autoradiography was made. Autoradiographs of both bulk and crushed samples showed presence of regions with high activity superposed on uniformly high background. However, examination of the "hot" spots using optical microscopy and X-ray fluorescence mapping failed to reveal the carrier phases, only Fe-containing metal chips, most likely, derived from the sampling tools, were found.

Scanning electron microscopy was the main method to search for the fuel-related particles and to address their properties. The samples of block graphite were studied in as-received state after mechanical crushing and after the leaching. The graphite matrix showed no impurities in concentrations above detection limits (~0.1–0.3%). Typical image of the sample is shown in Fig. 5a. The specimen surface is covered by large number of foreign phases, most of them are Al–Mg–silicates; quasispherical morphology of some particles resembles zeolites (Fig. 5b). Aluminosilicate inclusions in nuclear graphite from similar reactors were reported earlier[26]. Such inclusions may undergo various transformations during reactor operation. Their morphology and, eventually, composition might approach that of precipitates observed in the current work, but in any case, the precipitates are much more abundant than the inclusions. Morphology, size, and composition of the foreign phases found in the current work drastically differ from precipitates formed on surface of i-graphite soaked in model ground water for 1–2 years[26]. In the first 10–15 years of the reactor operation, accidents involving leaks of filtered river water used for cooling were rather frequent. We believe that contamination of graphite by suspended minerals and colloids from the leaked fluids is responsible for the precipitation of foreign phases.

After the leaching amount of the precipitates apparently decreased, but it is uneasy to quantify differences between

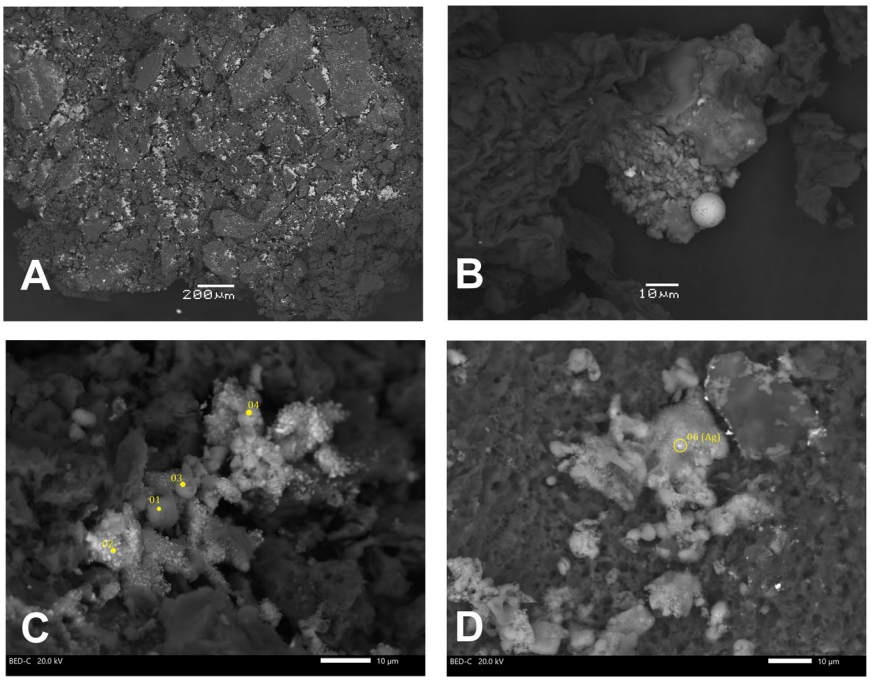

Fig. 5 Scanning electron microscopy of the graphite sample after leaching, BSE mode. A General view. **B** Quasispherical natural zeolite particle. **C**, **D** Typical aluminosilicate precipitates. **D** A precipitate with Ag admixture. Scale bars: 200 µm in (**A**); 10 µm in (**B**–**D**).

as-received and leached graphite samples (see also Discussion). In addition, after the leaching numerous AgCl particles with sizes less than few µm appeared (Fig. 5d). Laboratory contamination is excluded and, taken into account γ-spectroscopy data, we believe that detected Ag is a FP released from the fuel debris. After the leaching zeolite-like phases and the AgCl particles often contain 0.07–2 at% of Cs (semiquantitative values).

The absolute majority of phases on graphite were represented by aluminosilicate minerals and, in rare cases, metal chips from the extraction tools. After dedicated search fuel-derived nuclides were found in some mineral precipitates. We emphasize that with few exceptions such particles were unremarkable even in the back-scattering detection mode. The absolute majority of them are just few microns in size with irregular, "molten" morphology (Fig. 6). EDX spectra reveal presence of fuel-related elements, i.e., uranium, sometimes Pu and FP such as noble metals (Pd, Ru), rare earth elements (REE: Ce, Pr, Nd, Gd), Ba, Sr, Tc, Mo, Zr. In some cases, morphologically well-formed crystals are observed on surfaces of the "amorphous" aluminosilicates; these crystals generally do not contain fuel debris (Fig. 6a). Spatial distribution of fuel-derived elements in the Al–Si carriers is highly heterogeneous on micron scale; we also recall that difference in BSE contrast between the radionuclide-bearing and barren particles is only marginal, if any at all. It is likely that the Al–Si grains may preferentially attach to cracks in graphite and promote its mechanical destruction. Figure 6e shows an example of a graphite parallelepiped approximately 300 × 100 × 20 µm in size, which was fractured by gentle mechanical action revealing numerous inclusions. The fuel-derived elements are occasionally detected in defects of graphite pieces (Fig. 7). Composition of such domains is dominated by elevated uranium (up to 59 at%), Pu (up to 5.9%), REE, Ru, and Pd. Elements as Al, Si, and Fe are always present, but relative enrichment with fuel debris is high. Such domains may represent deposits of colloidal particles or pre-existing Al–Si–Fe inclusions[26]. Transport of U/Pu in superheated steam is also possible[27,28], although this mechanism is not very important.

Close association of fuel debris and Al–Si minerals can be explained by very weak retention of dispersed fuel debris on surface of graphite blocks and removal of the attached fragments by fluids flows during the accident itself and related countermeasures. However, if fuel debris contacts pre-existing of newly deposited silicates, which wet graphite, they remain in the pile. In some cases, residual heat release and heating of the debris during subsequent irradiation could have been sufficiently intense for partial melting of the Al–Si phases, thus explaining their "molten" appearance.

Despite all limitations due to irregular morphology, small size and unknown contribution of graphite matrix allowed semiquantitative analysis and interelement correlations were established (Fig. 8). To facilitate comparison all measured concentrations were normalized to uranium. Although in total more than 60 regions were studied, the compositional fields are likely broader. Several groups of debris particles can be distinguished based on the correlations. On plots of Pd/Ru vs. Pu (Fig. 8a, b) two markedly different trends are observed: with positive and with negative correlations between these elements. The negative trend is mostly observed on as-received graphite, however, the effect of leaching on platinum group elements should be minor and certain bias may be present due to smaller number of analyses on the as-received specimen. For the as-received graphite Pd and Ru are highly correlated (Fig. 8b). For the leached specimen the correlation is less obvious; also particles with very high Ru content (up to 80% of U content), are found. In general, Ru/U ratio changes in broad range from 0.06 to 189. For particles possessing close amount of Pu concentration of ruthenium varies widely, which could be explained by Ru volatilization from some of the precipitates. This hypothesis is supported by positively correlated Ru and Mo (Fig. 8f)—elements readily forming volatile compounds.

On plots of REE (here Ce and Nd) vs. Pu (Fig. 8g, h) two groups of points with different slopes are distinguished. The same analysis points also group on REE-Ru and REE-Zr plots. We note that spatial position of analytical points belonging to the either group on graphite surface is chaotic and particles with markedly different composition may be separated by few microns only. Good positive Ce–Zr correlation is observed (Fig. 8h). Two populations of particles differing in Ce content are distinguished. Zirconium and plutonium are always negatively correlated (Fig. 8e). Based on limited statistics (three analyses) there could be a positive Tc–Mo trend.

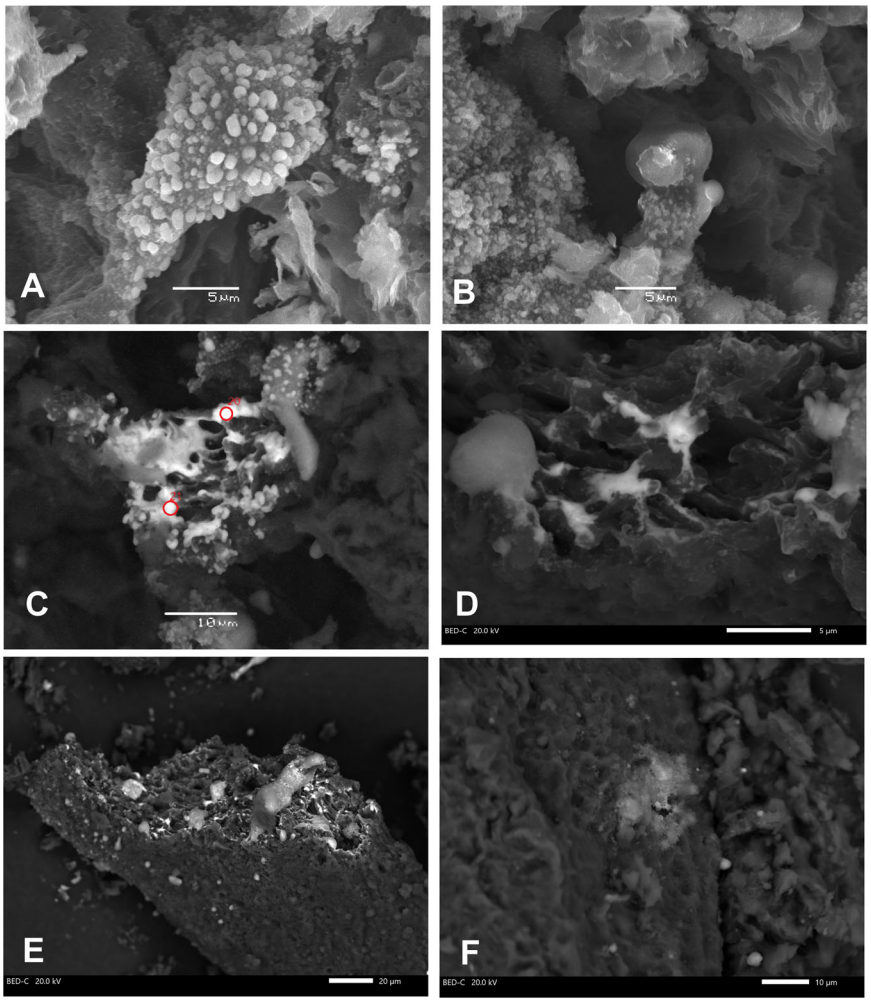

Fig. 6 Scanning electron microscopy of the graphite sample. Blue circles indicates some analysis spots with fuel debris, Red ones—pure aluminosilicates. Scale bars: 5 µm in (**A**, **B**, **D**); 10 µm in (**C**, **F**); 20 µm in (**E**).

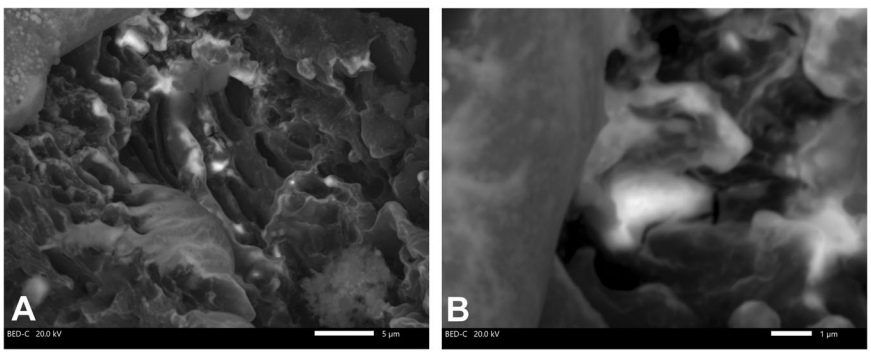

Fig. 7 Scanning electron microscopy of the spots fuel debris smeared on graphite matrix (bright spots in the center, see text for detail). Scale bars: 5 µm in (**A**); 1 µm in (**B**).

Some particles are compositionally unusual, for example, a Cs–Ba particle (Fig. 8c, d). This particle also contains uranium, which allows to distinguish it from natural zeolites. Sr–Ba "hot" particles are not uncommon in spent fuel and were found, for example, in Chernobyl NPP fallout[29].

DISCUSSION

Presence of significant amount of FPs is expected for high burn-up fuel. Yield of FPs depends both on neutron spectrum and on parent nuclide (^{235}U or ^{239}Pu). Behavior of FPs depends on oxygen potential and differ considerably in metal and ceramic fuel due to both contrasting crystal chemistry and microstructure of these materials[30,31]. In metal fuel lanthanides are insoluble in the matrix and mainly segregate in pores, cracks and in fuel-cladding gap; whereas platinum group elements, Zr and Pu form solid solutions. Concentration gradients across blocks of metal fuel is a well-known phenomenon influencing, among other factors, melting temperature, kinetics, and extent of the fuel-cladding reactions[32]. In particular, due to the temperature gradients and

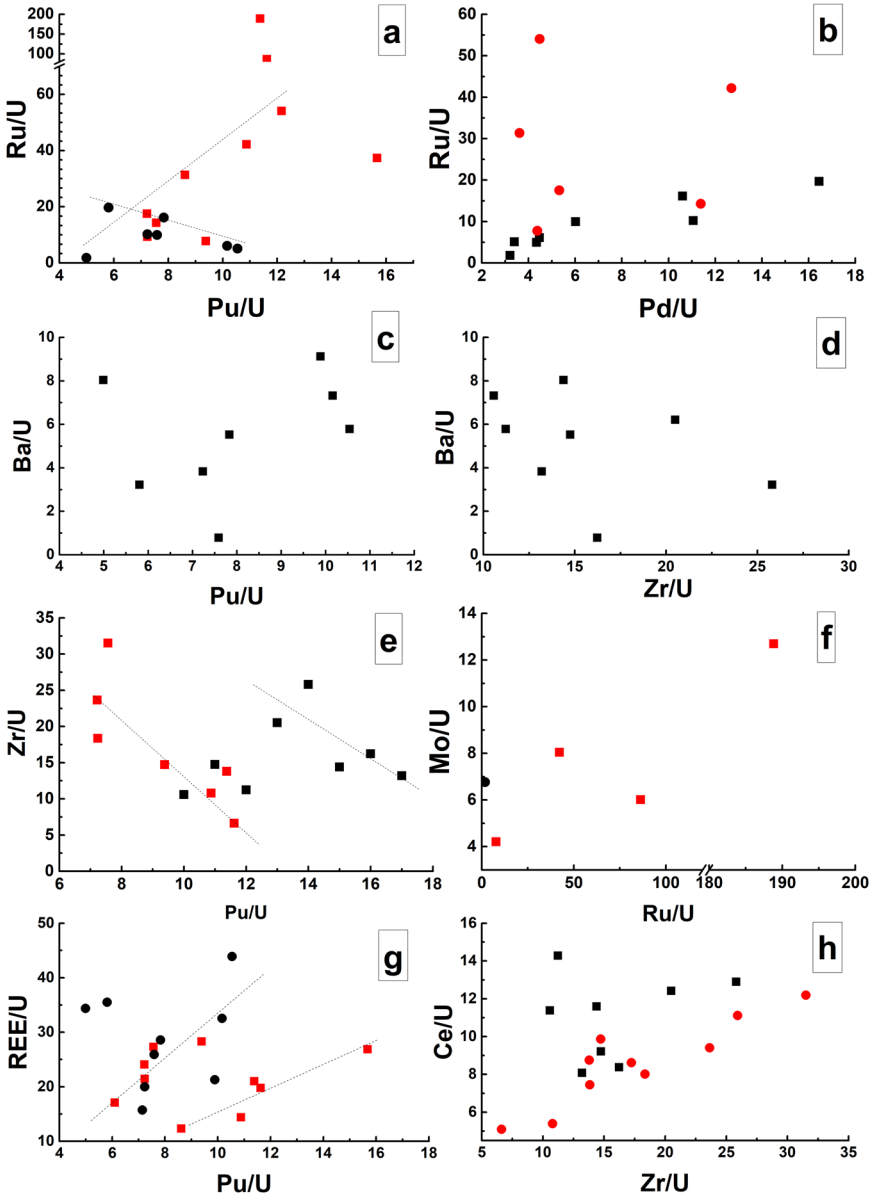

Fig. 8 Interelement correlations for fuel debris particles. Concentrations of all elements (fission products) are normalized to U content to compensate semi-quantitative character of the measurements (see text for detail). **A**, **B** Platinum group elements (Pd, Ru) plotted vs. Pu each other, respectively. **C**, **D** Barium as a function of Pu and Zr contents. **E** Zr vs. Pu. **F** Mo vs. Ru. **G**, **H** Rare Earth elements (REE) plotted vs. Pu and Zr, respectively. Black symbols—as received graphite, red—leached sample. The lines are drawn to guide an eye to possible trends.

markedly different solubilities of Pu and Zr in various polymorphs of metallic uranium, the Pu/Zr ratio may change considerably along a profile from the fuel block center to its periphery[31,33]. Presumably, the fuel debris particles forming two groups on the Pu–Zr plot (Fig. 8e) may be explained by formation from domains of a fuel block with different extent of the fuel–cladding interaction.

Campaigns of the studied reactor were short and most likely the main fraction of FPs and actinides was formed after the accident, i.e., after destruction of the fuel channels and fuel dispersion. Consequently, interpretation of composition of the fuel debris is complicated by uncertainties in the irradiation conditions and by unknown details of radionuclides transport in course of the accident and subsequent reactor operation. Although the main volume of the reactor core is in reducing conditions, locally oxidized environment may be formed influencing speciation of radionuclides and their carriers. In addition, oxidation leads to evolution of porous structure and wettability of the graphite itself, thus affecting retention of the mineral phases. Kinetics of graphite oxidation in presence of steam strongly depends on temperature and hydrogen formation due to radiolysis, but below 800 °C these factors are not very important[34]. In course of routine reactor operation total porosity of graphite does not change considerably and share of closed pores is minor[20]. However, behavior of graphite oxidized during accident in radiation fields is poorly constrained and requires detailed investigation.

Efficiency of graphite decontamination is a crucial factor for reactor decommissioning. It is highly likely that although transport of volatile forms was possible, the studied graphite was not in contact with water after the accident. Such assumption explains non-negligible, albeit incomplete, leaching of radionuclides in the laboratory (Fig. 5). However, estimation of the laboratory leaching effect on chemistry of fuel debris particles is an ambiguous task. Although at least 25 uranium-containing regions were studied on every sample and

different interelement correlations are found in initial and leached graphite, it is likely that the compositional fields overlap. In our opinion, the leaching of certain elements and radioisotopes in the laboratory experiments is not the main reason for broadness of the compositional range. Rather, the difference of the initial and leached samples is mostly explained by changes of accessible surfaces, in particular, by exposure of voids and cracks during mechanical crushing of the fragile leached sample for the SEM study. Behavior of molybdenum is a good marker of the leaching losses. Mo makes at least 40% of FPs, but it is strongly depleted in the studied samples. Since Mo is readily leached from fuel debris in broad redox range[35], the depletion is well explained. In the same time, platinum group elements are poorly soluble in aqueous solutions.

Although relative fraction of the fuel-contaminated graphite in most reactors is not high, results of the current work shows that activity of actinides in such material may reach up to 10^6 Bq/g. The major fraction of radionuclides is located in boundaries between the graphite blocks and cracks and is closely associated with aluminosilicate particles originating from coolant and flushing solutions employed for mediation of the LOF accidents. Upon prolonged contact with aqueous fluids, significant fraction reaching several tens of percent of major actinides may be released into environment. This indicates that retention of fuel-related radionuclides in i-graphite contaminated by fuel debris is relatively poor and is insufficient for long-term storage. Consequently, development of repository strategy should include means to prevent significant loss of radionuclides. The "on-site storage" approach implies construction of suitable engineering barriers. As shown on model systems[36] and in practical case of dismantling of Uranium-graphite reactor EI-2[37] such barriers can be made. In case of full dismantling of the pile and deposition of i-graphite with fuel residues in a repository, it is necessary to develop methods of decontamination and/or immobilization of the graphite into waste forms.

METHODS

Samples preparation

Samples preparation for characterization is briefly described below, for details see Supplementary methods. For initial assessment of presence of fuel debris selected fragments were mechanically dispersed either by an end cutter (for the sleeve) or by abrasion (for the block fragments) and sieved to extract the <0.2 mm fraction (Fig. S1c). After homogenization the powder was separated into representative batches for measurements of γ-activity of ^{137}Cs and ^{241}Am. In total ~20 g of the sleeve graphite and ~1 g were analyzed.

Leaching experiments

The leaching experiments were performed on a sample from graphite block. The fragment with irregular shape was placed into a hermetic polypropylene vial filled with contact solution. Composition of the solution (in mg/l) is: Na^+ 87.1, Mg^{2+} 9.12, Ca^{2+} 35.1, HCO_3^- 231.1, SO_4^{2-} 36.4, Cl^- 62.5, pH 8.5; it matches ground waters of Nizhnekansky massif, Russia, where construction of geological repository of nuclear waste is planned. The experiment was performed at 25 °C. The solution was replaced and analyzed after 1, 14, 45, 90, 150 days; total duration was 300 days. Actinides in every batch of the contact solution were measured using low-background ALPHA-ARIA (AMETEK) spectrometer after pre-concentration and separation. Concentration of γ-active nuclides was measured using HPGe GEM-10P detector (Ortec). The sample is measured on a special holder fixed on the detector axis at a given height to assure proper and reproducible measurement geometry. The sample for γ-spectrometry consisted of a ≤1 mm thick layer of finely dispersed graphite powder placed into polyethylene vial 8 mm in diameter with 0.5 mm thick walls.

Measurements of thermomechanical properties

Density, thermal conductivity and mechanical strength were measured on cylindrical samples 10 mm high and 8 mm in diameter. The density and porosity (total as well as open and closed) were measured by hydrostatic method according to Russian standard GOST 18898-89 "Powder products. Methods of determination of density, oil content and porosity" with a 1.5% uncertainty. The thermal conductivity was measured using stationary axial thermal flow method; the uncertainty is 10%. Tensile strength was measured in direct compression mode with acquisition of "load-deformation" curve; the uncertainly is 10%.

Electron microscopy

Scanning electron microscopy was performed both on as-received block graphite and after the leaching. Conductivity of the graphite made additional coating obsolete. JEOL JSM-6480LV Scanning Electron Microscope equipped with a W thermal emission cathode and an Oxford X-Max^n 50 detector was used. The accelerating voltage was 20 kV; electron beam current—10 nA. The XPP correction was applied using Oxford Instruments INCA software, but precise quantitative analysis of observed phases is impossible due to small size of the particles and irregular morphology. Although some of elements (or fraction of them) may be present in metallic form, oxides were assumed in all calculations.

Raman spectroscopy

Raman spectra of a sample of a virgin GR-220 graphite and samples identical to those employed for the SEM studies were acquired using Renishaw inVia spectrometer in quasi back-reflection geometry. Spectra were recorded using 405 and 633 nm excitation.

DATA AVAILABILITY STATEMENT

The datasets generated during the current study such as results of electron microprobe analysis are available from the corresponding author on reasonable request.

Received: 19 June 2021; Accepted: 24 February 2022;
Published online: 23 March 2022

REFERENCES

1. Processing of Irradiated Graphite to Meet Acceptance Criteria for Waste Disposal. Results of a Coordinated Research Project (International Atomic Energy Agency, TECDOC Series, 1790).
2. The European Commission "CAST (CArbon-14 Source Term)" Project—A Summary of the Main Results from the Final Symposium. *Radiocarbon* **60**, 1649–1923 (2018).
3. Bushuev, A. V. et al. Quantitative determination of the amount of ^{3}H and ^{14}C in reactor graphite. *Atomic Energy* **73**, 959–962 (1992).
4. Girke, N. A. et al. ^{14}C in spent graphite from uranium-graphite reactors at the Siberian chemical combine. *Atomic Energy* **112**, 63–66 (2012).
5. Volkova, A. G., Zakharova, E. V., Pavlyuk, A. O. & Shiryaev, A. A. Radionuclides in irradiated graphite of uranium–graphite reactors: decontamination of sleeves using liquid reagents. *Radiochemistry* **60**, 558–562 (2018).
6. Volkova, A. G., Zakharova, E. V., Rodygina, N. I., Pavlyuk, A. O. & Shiryaev, A. A. Radionuclides in irradiated graphite of uranium–graphite reactors: decontamination by thermochemical methods. *Radiochemistry* **60**, 657–663 (2018).
7. Bushuev, A. V. et al. Experimental determination of the spent graphite radioactive contamination at plutonium-production reactors of the Siberian Group of Chemical Enterprises (Tomsk-7). *Nucl. Technol.* **140**, 51–61 (2002).
8. Bushuev, A. V. et al. Fission products and actinides in spent graphite masonry of the reactors at the Siberian Chemical Combine. *Atomic Energy* **89**, 650–657 (2000).
9. Bushuev, A. V. et al. Radioactive contamination of spent reactor graphite. *Atomic Energy* **117**, 196–200 (2015).
10. Bulanenko, V. I. & Frolov, V. V. Radiation characteristics of fuel residues in the graphite stacks of decommissioned uranium-graphite reactors. *Atomic Energy* **78**, 382–385 (1995).
11. Pomfret, D. G. Safety and dose management during decommissioning of a fire damaged nuclear reactor, in *IRPA-10 Proceedings of the 10th international congress of the International Radiation Protection Association on harmonization of radiation, human life and the ecosystem*, No, T-2-2, P-5-299. (Japan Health Physics Society, Tokyo, 2000).
12. Dorofeev, A. N. et al. On reactor graphite disposal. *Radioact. Waste* **7**, 18–30 (2019).
13. Bylkin, B. K. et al. Induced radioactivity and waste classification of reactor zone components of the Chernobyl Nuclear Power Plant Unit 1 after final shutdown. *Nucl. Technol.* **136**, 76–88 (2001).

14. Pavlyuk, AO., Zagumennov, V. S., Kotlyarevskii, S. G. & Bespala, E. V. Thermodynamic simulation of equilibrium composition of reaction products at dehydration of a technological channel in a uranium-graphite reactor. *Therm. Eng.* **65**, 61–67 (2018).
15. Channel-type nuclear power reactor RBMK. (eds. Cherkashov, Yu. M., Nikitin, Yu. M., Stenbok, I. A.) (NIKIET, Moscow, 2006).
16. Krinitsyn, A. P. & Pazukhin, E. M. Investigation of graphite samples from 4th unit of Chernobyl NPP. I. Radiocaesium in graphite and peculiarities of its behavior. Evaluation of amount of expelled carbon-14. *Radiokhimiya* **36**, 522–528 (1994).
17. Bulanenko, V. I., Frolov, V. V. & Nikolaev, A. G. Radiation characteristics of graphite removed from operation in uranium-graphite reactors. *Atomic Energy* **81**, 743–745 (1996).
18. Bushuev, A. V., Zubarev, V. N. & Proshin, I. M. Impurity composition and content in graphite from commercial reactors. *Atomic Energy* **92**, 331–335 (2002).
19. Kane, J. J., Carroll, M., Windes, W. E. International Nuclear Graphite Specialists' Meeting INGSM-17, (IAEA, 2016).
20. Pavlyuk, A. O. et al. Determination of parameters of porous structure affecting the release mechanisms of long-lived radionuclides from irradiated graphite in contact with liquid media. *Radiochemistry* **62**, 759–768 (2020).
21. Goncharov, Yu. S., Virgiliev, V. D., Rodchenkov, B. S. Russian reactor graphites and their use in stacks of nuclear reactors. (NIKIET, Moscow, 2013).
22. Shiryaev, A. A. et al. Radionuclides in irradiated graphite of industrial uranium–graphite reactors: effect of irradiation and thermochemical treatment on the graphite structure. *Radiochemistry* **60**, 657–663 (2018).
23. Smith, M. W. et al. Structural analysis of char by Raman spectroscopy: Improving band assignments through computational calculations from first principles. *Carbon* **100**, 678–692 (2016).
24. Krishna, R., Jones, A. N., Edge, R. & Marsden, B. J. Residual stress measurements in polycrystalline graphite with micro-Raman spectroscopy. *Radiat. Phys. Chem.* **111**, 14–23 (2015).
25. Pavlyuk, A. O., Kotlyarevskii, S. G., Kan, R. I., Volkova, A. G. & Zakharova, E. V. Study of the Process of Leaching of Long-Lived Radionuclides ^{14}C and ^{36}Cl from Irradiated Graphite. *Radiochemistry* **63**, 187–196 (2021).
26. Shiryaev, A. A., Volkova, A. G., Dvoryak, S., Nickolsky, M. S. & Zakharova, E. V. Influence of long-term aqueous leaching of irradiated graphite on surface properties and behavior of radionuclides. *MRS Adv.* **5**, 177–184 (2020).
27. Krikorian, O. H., Fontes, A. S., Ebbinghaus, B. B. & Adamson, M. G. Transpiration studies on the volatilities of $PuO_3(g)$ and $PuO_2(OH)_2(g)$ from $PuO_2(s)$ in the presence of steam and oxygen and application to plutonium volatility in mixed-waste thermal oxidation processors. *J. Nucl. Mater.* **247**, 161–171 (1997).
28. Meschter, P. J., Opila, E. J. & Jacobson, N. S. Water vapor–mediated volatilization of high-temperature materials. *Annu. Rev. Mater. Res.* **43**, 559–588 (2013).
29. Devell, L. Nuclide composition of Chernobyl hot particles. In: Von Philipsborn H. and Steinhausler F. (eds.). Hot particles from the Chernobyl fallout. Proceedings of an International Workshop held in Theuern 28/29 October 1987. *Schriftenreihe des Bergbau- und Industriemuseums Ostbauern Theuern*, 16, 23-34 (1988).
30. Ogata, T. Metal Fuel, in: Comprehensive Nuclear Materials, Editor(s): Rudy J. M. Konings, Elsevier, 2012, Pages 1-40.
31. Kleykamp, H. Chemical state of the fission products in oxide fuels. *J. Nucl. Mater.* **131**, 221–246 (1985).
32. Keiser, D. D. Metal fuel-cladding interaction. In (eds Rudy J. M. Konings) *Comprehensive Nuclear Materials*. (Elsevier, 2012).
33. Kim, Y. S., Hofman, G. L., Hayes, S. L. & Sohn, Y. H. Constituent redistribution in U–Pu–Zr fuel during irradiation. *J. Nucl. Mater.* **327**, 27–36 (2004).
34. Goncharov, V. V. et al. Deistvie oblucheniya na grafit yadernykh reaktorov. *Action of Irradiation on Nuclear Reactor Graphite*. (Atomizdat, Moscow, 1978).
35. Cui, D., Eriksen, T. & Eklund, U.-B. On metal aggregates in spent fuel, synthesis and leaching of Mo-Ru-Pd-Rh alloy. *Mater. Res. Soc. Symp . Proc.* **663**, 427 (2001).
36. Pavliuk, A. O., Kotlyarevskiy, S. G., Bespala, E. V. & Zakharova, E. V. Experimental simulation of the radionuclide behaviour in the process of creating additional safety barriers in solid radioactive waste repositories containing irradiated graphite. *IOP Conf. Ser. Mater. Sci.* **142**, 1–8 (2016).
37. Pavliuk, A. O. et al. Experience of on-site disposal of production uranium-graphite nuclear reactor. *J. Environ. Radioactivity* **184-185**, 22–31 (2018).

ACKNOWLEDGEMENTS

Analytical measurements were performed using equipment of Center of Joint use of IPCE RAS. We thank Mr. A.Averin for assistance in Raman measurements.

AUTHOR CONTRIBUTIONS

A.O.P., S.G.K., and R.I.K.—sample acquisition and preparation, investigations of the pile, thermomechanical measurements; A.G.V., E.V.Z., V.O.Y., and A.A.S.—leaching, microstructural investigations. All authors participated in data analysis and interpretation, paper preparation and writing.

COMPETING INTERESTS

The authors declare no competing interests.

ADDITIONAL INFORMATION

Supplementary information The online version contains supplementary material available at https://doi.org/10.1038/s41529-022-00235-3.

Correspondence and requests for materials should be addressed to Andrei A. Shiryaev.

Reprints and permission information is available at http://www.nature.com/reprints

Publisher's note Springer Nature remains neutral with regard to jurisdictional claims in published maps and institutional affiliations.